Transition-metal Saccharide Chemistry and Biology: Synthesis, Characterisation, Redox Behaviour, Biointeraction and Data Correlations of Dinuclear Chromium(III) Complexes

Sharada P. Kaiwar, M. S. Srinivasa Raghavan and Chebrolu P. Rao*
Bioinorganic Laboratory, Department of Chemistry, Indian Institute of Technology, Powai, Bombay 400 076, India

A series of dinuclear chromium(III) complexes has been synthesised by reduction of chromate by a variety of saccharides and related compounds. The complexes have been characterised by various analytical (elemental and ICP-AES analysis, TLC, HPLC) and spectroscopic (UV/VIS, FTIR, EPR, ^1H and ^{13}C NMR) methods. Antiferromagnetic interactions between the two Cr^{III} centres have been established by magnetic susceptibility measurements and the hydrolytic stability and redox behaviour of the complexes have been established by extensive electrochemical studies which gave several correlations. The interaction of some of the complexes with DNA has been studied by gel electrophoresis.

Chromium, particularly in its +6, +5 and +3 oxidation states, has become an important element in bioinorganic chemistry even though it has no demonstrated positive role in biological systems. However, chromium is known to be toxic to biological cells in its +6 oxidation state and also an ecological hazard. Cellular functions are believed to be impaired as a result of the uptake of tetrahedral, anionic Cr^{VI} units by biological cells followed by its reduction and the possible formation of Cr^{III} cross-linked products by the cellular components. Recent solution studies of Cr^{VI} reduction by a variety of cellular-mimicking molecules shed light on mechanistic aspects and also on their relative reactivities.[1-3] The Cr^{VI}-reducing ability of OH- and COOH-containing molecules has resulted in the formation of Cr^{III} products *via* long-lived Cr^{V} intermediate species. These are, in turn, capable of exchanging and expanding co-ordination rapidly, which may be an important factor rendering chromium an ecologically hazardous element. While a large number of solution studies have been performed to explain several of these aspects, little has been reported on the solid-state isolation and characterisation of the final Cr^{III} products.

As the saccharides and their derivatives are indispensible in biological and ecological systems and these coexist with transition metal ions, there has recently been some concern regarding their interactions. In an ecological context, organic chelating agents in soil can have two opposing effects on toxic metal ions: either they can promote solubilisation and movement of the metal ions, thereby increasing their toxicity, or they can sequester the toxic metal ion and make it less available to the plant.[4] This demands the development of bioco-ordination chemistry of transition-metal ions with molecules containing –OH and –COOH functions such as saccharides and their derivatives. While interactions between saccharides and alkali and alkaline-earth metal ions, and also other non-transition-metal cations, is well documented in the literature, transition-metal saccharide interactions remain largely unexplored.[4-9] In spite of the presence of a large number of hydroxyl groups in saccharide molecules, their poor complexing ability with metal ions can be attributed to their high pK_a values. However the interaction of amine complexes of Co^{3+} and Ni^{2+} with saccharides gave crystalline products in low yields with co-ordinated glycosides as reported by Yano.[7] Although the use of several Cr^{VI} salts in the synthesis of sugar derivatives has become routine,[10] the exact nature of the ultimate Cr^{III} product formed in these reactions has largely been unexplored. As an ongoing project, we have synthesised a large number of transition-metal–saccharide complexes.[11-20] In this paper we report the syntheses and isolation of Cr^{III} complexes generated *via* chromate reduction by saccharides and their derivatives and the characterisation of these complexes by spectroscopic, magnetic, electrochemical and other analytical techniques and some interesting correlations have been identified. Some of the Cr^{III} products have been tested for their reactivity with DNA.

Experimental

Syntheses.—The Cr^{III}–D-*Ribose Complex* **1**. An aqueous solution (25 cm^3) of potassium chromate (1.942 g, 10 mmol) was added to an aqueous solution (75 cm^3) of D-ribose (D-Rib) (10.8 g, 60 mmol) and the resultant solution was purged for 20 min with N_2 and stirred at 40–45 °C for about 7 d. Completion of the reaction was monitored by UV/VIS absorption and EPR spectra measured at various time intervals.[12] The solution was then filtered, concentrated and precipitated using MeOH to give a green product which was washed with warm methanol. The product was further purified by stirring for 1 d in hexane (25 cm^3) and filtering, and the process was repeated. The compound was finally washed with diethyl ether and dried under N_2. The filtrate, upon slow evaporation, yielded a white organic solid that does not contain any chromium.

A similar procedure was adopted to synthesise other Cr^{III} saccharide and related complexes, except those of ethylene glycol (ethane-1,2-diol, edo) and glycerol (propane-1,2,3-triol, pto). The saccharides and their derivatives used, which formed complexes **1**–**16** were the pentoses D-Rib (**1**) and D-xylose (D-Xyl) (**2**), the disaccharides D-lactose (D-Lac) (**3**) and D-maltose (D-Mal) (**4**), the alcohols edo (**5**), pto (**6**), mannitol (Man-ol) (**7**), dihydroxyacetone (dha) (**8**), and adenosine triphosphate (ATP) (**9**), D-glucose (D-Glc) (**10**), D-fructose (D-Fru) (**11**), D-galactose (D-Gal) (**12**), D-mannose (D-Man) (**13**), L-sorbose (L-Sor) (**14**), D-galacturonic acid (D-GalA) (**15**) and D-gluconic acid (D-Glc-onic) (**16**). The chromate to ligand ratios used were 1:6 for complexes **1**, **2**, **7** and **8** and 1:4 for **3**, **4** and **9**. For **5** and **6** the reactions were carried out in neat reductants with a chromate to reductant ratio of *ca.* 1:100. The yields for the corresponding

Cr^{III} complexes were found to be in the range 55–76% based on chromium. The time for the completion of the reaction was typically in the range 5–30 d, depending upon the reductant used. Some details of the complexes **10–16** have already been reported.[20]

Characterisation. Final, purified products were characterised by several routine analytical, spectroscopic, electrochemical and magnetic techniques. The compounds are hygroscopic and hence special precaution is necessary while handling. Carbon and hydrogen contents were analysed on an automatic Carlo Erba 1100 CH analyser, metal contents by inductively coupled plasma atomic emission spectroscopy (ICP-AES). The UV/VIS absorption studies were carried out on a Shimadzu UV-260 spectrophotometer using a 1.0 cm cell in the range 400–850 nm and a 0.1 cm cell in the range 190–400 nm. Thermogravimetric analyses of the complexes **1**, **4**, **5**, **10**, **11** and **16** were carried out on a Dupont 9900 instrument under an N_2 atmosphere up to 1000 °C. Fourier-transform IR (FTIR) spectra were recorded in a KBr matrix on a Nicolet spectrometer, and EPR spectra were measured both in solution and in the solid state on a Varian ESR-112 spectrometer with tetracyanoethylene (tcne) as the field marker (g = 2.002 77). Variable-temperature magnetic susceptiblity measurements of the solid samples were performed on a Faraday balance, cyclic voltammetric (CV) studies on a BAS 100B electrochemical analyser using a hanging drop mercury electrode (HMDE) or a platinum electrode as working electrodes and Ag–AgCl as reference electrode using 0.1 mol dm^{-3} NMe_4Cl as supporting electrolyte. Proton and ^{13}C NMR spectra were recorded on a Varian XL-300 spectrometer. Conductivity studies were performed with millimolar aqueous solutions of the complexes. The purity of the complexes was checked by thin-layer silica gel chromatography with a mobile phase of water–acetone–butanol (10:4:4), or by HPLC (for **10**) using a reverse phase column, with water as eluent. Although the ATP complex, **9**, was obtained as a green solid it could not be fully characterised due to its highly hygroscopic nature.

Found: C, 29.10; H, 4.35; Cr, 12.90; K, 4.75. $C_{20}H_{31}Cr_2KO_{23}\cdot 2H_2O$ (complex **1**) requires C, 29.35; H, 4.30; Cr, 12.70; K, 4.75. Found: C, 29.70; H, 4.25; Cr, 12.95; K, 4.70. $C_{20}H_{31}Cr_2KO_{23}\cdot H_2O$ (**2**) requires C, 30.00; H, 4.15; Cr, 13.00; K, 4.90. Found: C, 31.70; H, 4.65; Cr, 11.40; K, 4.30. $C_{24}H_{35}Cr_2KO_{25}\cdot 2H_2O$ (**3**) requires C, 31.95; H, 4.30; Cr, 11.55; K, 4.30. Found: C, 32.40; H, 4.50; Cr, 11.65; K, 4.20. $C_{24}H_{35}Cr_2KO_{25}\cdot H_2O$ (**4**) requires C, 32.60; H, 4.20; Cr, 11.75; K, 4.40. Found: C, 20.15; H, 3.60; Cr, 21.45; K, 8.10. $C_8H_{11}Cr_2KO_{11}\cdot 3H_2O$ (**5**) requires C, 20.00; H, 3.55; Cr, 21.65; K, 8.15. Found: C, 28.10; H, 4.60; Cr, 13.70; K, 9.95. $C_{18}H_{32}Cr_2K_2O_{20}\cdot H_2O$ (**6**) requires C, 28.15; H, 4.45; Cr, 13.55; K, 10.15. Found: C, 30.90; H, 5.35; Cr, 11.05; K, 4.05. $C_{24}H_{43}Cr_2KO_{25}\cdot 3H_2O$ (**7**) requires C, 31.05; H, 5.30; Cr, 11.20; K, 4.20. Found: C, 18.55; H, 3.60; Cr, 16.00; K, 18.05. $C_{10}H_{21}Cr_2K_3O_{13}\cdot 4H_2O$ (**8**) requires C, 18.70; H, 3.25; Cr, 16.20; K, 18.20.

DNA Binding Studies.—Agarose gel (0.7%) was prepared to which samples were applied in 1X TEB buffer [0.05 mol dm^{-3} tris(hydroxymethyl)aminomethane (Tris) hydrochloride, 0.05 mol dm^{-3} boric acid, 1 mmol ethylenediaminetetraacetic acid (H_4edta), pH 8.0 containing 1 μg cm^{-3} ethidium (3,8-diamino-5-ethyl-6-phenylphenanthridinium) bromide]. Each aliquot contained 0.92 mol dm^{-3} (for complex **1**) or 1.04 mol dm^{-3} (for **3**) solution (10 μl) of Cr^{III} product (on moving towards the right on the gel the Cr^{III} product concentration decreased by an order of magnitude as compared to the one previous), 10 μl of 20 ng μl^{-1} pSV_2neo plasmid DNA and 5% 'Dye glycerol' [1% Bromophenol Blue in sterile distilled water and an equal volume of glycerol (nuclease free)] and electrophoresis was carried out at 85 V for 3–5 h. The gel was destained for 30 min in 1 mol dm^{-3} $MgSO_4$ and then photographed while illuminating with a 302 nm UV-transilluminator.

Results and Discussion

The ligands used in the chromate reaction were found not only to reduce the Cr^{VI} salts but also to complex the final Cr^{III} products. The final, purified, Cr^{III} products are highly soluble in H_2O, and are also soluble in several non-aqueous solvents such as MeOH, dimethyl sulfoxide (dmso), dimethylformamide (dmf) and to a lesser extent in MeCN in the presence of 18-crown-6 (1,4,7,10,13,16-hexaoxacycloctadecane). This may be attributed to the complexation of K^+ by the crown ether, thereby increasing the solubility in non-aqueous solvents. However, complex **6** is directly soluble in MeOH, dmso and dmf. The complexes were found to be pure and single components based on both the TLC and HPLC experiments.

(*a*) *Absorption Studies.*—Aqueous UV/VIS spectra of the final Cr^{III} products **1–9** in H_2O exhibited in general two d–d transitions, one in the range 556–604 nm [$A_{2g}(F) \longrightarrow T_{2g}(F)$] the other from 398–430 nm [$A_{2g}(F) \longrightarrow T_{1g}(F)$] with a weak shoulder at 695 ± 10 nm, together with one UV band in the range 196–212 nm arising from the ligand transition. Corresponding UV/VIS data is listed in Table 1. The spectra are typical of distorted octahedral Cr^{III} complexes.[11,12] Complexes **1–8** essentially exhibit similar spectra in different solvents with only marginal shifts (Table 1). The diffuse reflectance spectra in the range 300–800 nm of these complexes agree completely with the solution spectra showing that there is no dissociation of the complex units in solution.

Solution studies of complexes **1–8** in the pH range 2–12 showed only marginal changes in the ν_1 band position (a 5–12 nm blue shift at pH 2.0) and did not indicate any hydrolysis of the Cr^{III} centre, even at pH 2.0. The effect of various solvents and pH on these complexes is better understood from CV studies. In the visible region of the circular dichroism (CD) spectra, complexes **1–4** showed two d–d bands in the same position as in the absorption spectra.

The spectrum of the Cr^{III}–ATP complex **9** showed a band at 604 nm with shoulders at 430 nm and 683 nm consistent with the binding of the phosphate group in the final Cr^{III} product.[19] However, similar synthetic reactions attempted with adenosine monophosphate (AMP) and adenosine diphosphate (ADP) did not give isolable Cr^{III} products. This variation between ATP and AMP and ADP seems to be in accord with the optimal binding observed between magnesium and adenosine in triphosphate.[21]

(*b*) *FTIR Studies.*—The FTIR spectra of all the complexes exhibited features in the OH, CH and skeletal regions similar to those observed for other transition metal saccharide complexes.[5,12,20,22] The carboxylate groups exhibited a strong ν_{asym} band at around 1637–1650 cm^{-1} and a weak ν_{sym} band in the region 1430–1490 cm^{-1}, with $\Delta\nu$ < 200 cm^{-1}, suggestive of a loosely bound carboxylate group. As the FTIR spectra of complexes **1–4** synthesised from pure saccharides are very similar to those synthesised from saccharide acids,[20] the structures are likely to be similar. Complexes **5–8** also showed bands corresponding to the presence of oxidised ligands (1710 ± 10 cm^{-1} and 1690 ± 10 cm^{-1}) and H_2O (3416 ± 16 cm^{-1} and 1600 ± 10 cm^{-1}). Evidence for the oxidised groups is also found in the ^{13}C NMR spectra for the pentose and disaccharide complexes.

Ratios of the band areas for ν(O–H) and ν(COO^-) showed a linear correlation w.r.t. the number of K^+ counter ions for all the complexes [Fig. 1(*a*)]. A reasonably linear trend was also observed for the plot of ratio of the number of OH groups: the number of COO^- groups *vs.* the number of K^+ ions [Fig. 1(*b*)]. This may be because as the negative charge on the complex increases, the charge-neutralising K^+ counter ions preferentially bind the carboxylate group rather than the hydroxyls, thereby leaving many hydroxyl groups free.

Table 1 The UV/VIS data of complexes **1–9** in different solvents

Complex	Solvent	λ/nm (ε/dm³ mol⁻¹ cm⁻¹)
1	H_2O	706 (29), 571 (146), 408 (452), 332 (1077), 197 (26 618)
	MeOH	698 (31), 569 (134), 406 (483), 346 (898), 202 (28 371)
	dmf	698 (35), 574 (157), 416 (427), 332 (1002)
2	H_2O	706 (36), 556 (193), 416 (746), 328 (973), 196 (29 786)
	MeOH	704 (29), 564 (140), 544 (303), 406 (775), 346 (910), 286 (7575), 199 (47 661)
	dmf	700 (44), 557 (100), 404 (781), 340 (1532)
3	H_2O	696 (21), 575 (84), 414 (247), 334 (613), 201 (10 417)
4	H_2O	694 (29), 575 (73), 398 (421), 334 (614), 212 (8194)
	MeOH	698 (40), 571 (80), 404 (349), 346 (603), 306 (906), 209 (6951)
	dmf	706 (20), 583 (70), 410 (314), 368 (218), 342 (536)
5	H_2O	688 (13), 573 (70), 410 (114), 264 (1115), 209 (6951)
	MeOH	690 (12), 576 (73), 415 (116), 265 (1568), 217 (9677)
	dmf	700 (14), 578 (79), 416 (111)
	MeCN	700 (14), 574 (77), 411 (119), 278 (1168), 210 (14 974)
6	H_2O	706 (48), 586 (141), 414 (258), 342 (435), 200 (14 887)
	MeOH	718 (27), 584 (122), 409 (211), 203 (22 553)
	dmf	706 (33), 586 (103), 414 (177), 346 (311)
	MeCN	730 (25), 583 (126), 413 (192), 340 (454), 205 (17 168)
7	H_2O	706 (54), 594 (158), 417 (239), 274 (438), 197 (29 149)
	MeOH	706 (53), 593 (145), 417 (220), 216 (11 721)
	dmf	706 (50), 592 (187), 415 (278)
8	H_2O	704 (20), 579 (95), 406 (262), 326 (874), 215 (8966)
	MeOH	690 (27), 575 (86), 406 (212), 326 (793), 212 (7956)
	dmf	694 (22), 579 (87), 405 (223), 324 (709)
9	H_2O	683 (sh), 604, 430, 330, 257, 203

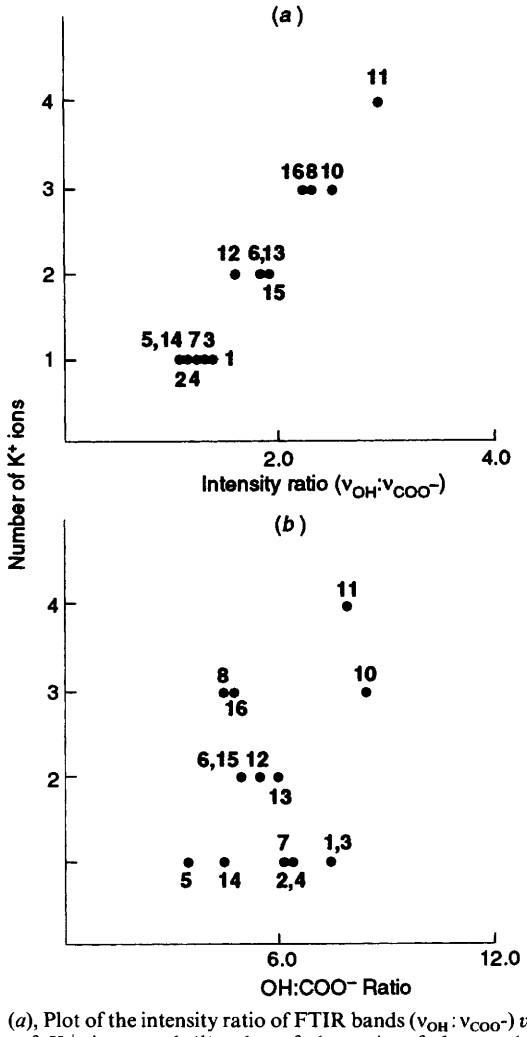

Fig. 1 (*a*), Plot of the intensity ratio of FTIR bands (ν_{OH}:ν_{COO^-}) *vs.* the number of K^+ ions; and (*b*), plot of the ratio of the number of OH:number of COO^- groups *vs.* number of K^+ ions. The numbers correspond to the Cr^{III} complexes given in Table 5

Table 2 EPR data and μ_{eff} values (298 K) for complexes **1–9**

Complex	Solution $g(\Delta\nu_{\frac{1}{2}}/mT)$	Solid $g(\Delta\nu_{\frac{1}{2}}/mT)$	μ_{eff}/μ_B
1	1.9735 (52)	1.9793 (62)	5.27
2	1.9765 (52)	1.9793 (65)	5.38
3	1.9624 (51)	1.9826 (53)	5.42
4	1.9708 (52)	1.9966 (54)	5.42
5	1.9765 (47)	1.9822 (54)	5.40
6	1.9678 (52)	1.9822 (54)	5.43
7	1.9706 (49)	1.9764 (59)	5.38
8	1.9734 (54)	1.9822 (59)	5.32
9	—	1.9735 (30)	—

(*c*) *EPR Studies.*—The X-band EPR spectra of complexes **1–9** showed a very broad band at $g \approx 2$ both in the solid state and in aqueous solution. The data (Table 2) are consistent with Cr^{III} being in an oxygen environment with distorted-octahedral geometry. Similar spectra were reported by Goodgame and co-workers[23] for ternary Cr^{III}–nucleotide–amino acid complexes. Surprisingly large linewidths in the range 20–40 mT were also noted for various Cr^{III} aqua species, which were attributed to zero-field splitting as they could not be fitted with other possible relaxation mechanisms. On the other hand, spectra of Fe^{III} saccharide complexes also exhibited broad bands at $g \approx 2$.[17,24] This, together with the solubility of these complexes in non-aqueous solvents in the presence of 18-crown-6, is indicative of the presence of extensive intermolecular interactions mediated through K^+ ions.

(*d*) *NMR Studies.*—As the proton NMR spectra of the complexes were very broad with the loss of fine structure, the specific assignment of each proton is not possible. As the synthetic reactions occur by chromate reduction, the saccharide ligands are oxidised to the corresponding carboxylic acid and are incorporated into the co-ordination sphere of the Cr^{III} products, as expected, as Cr^{III} is oxophilic. Spectra of complexes **5** and **6** showed the presence of an aldehyde group in the range δ 8–9. The proton NMR spectrum of complex **6** in dmso indicated the presence of a carboxylate function. The white products (not containing Cr^{III}) isolated from the syntheses of **1–3** and **7** exhibited ^1H NMR spectra consistent with the starting

Table 3 Thermogravimmetric analysis data for Cr^{III} complexes under a nitrogen atmosphere

Complex	Temperature/°C	Weight loss (%)	Possible molecules lost
1	97	4.0	$2H_2O$
	170	5.5	CO_2
	245	5.5	CO_2
	360	13.0	$6H_2O$
	485	20.0	6CO
	580	3.5	CO
	960	16.0	$3CO_2$
4	105	7.0	$H_2O + CO_2$
	137	3.0	CO
	215	2.0	H_2O
	330	15.0	$7H_2O$
	407	13.0	4CO
	502	13.0	4CO
	940	14.0	$3CO_2$
5	105	11.0	$3H_2O$
	235	3.5	H_2O
	375	17.0	$4.5H_2O$
	545	18.0	$2CO_2$
	817	6.0	CO
10	120	3.5	$2H_2O$
	265	8.7	$2CO_2$
	355	10.6	$6H_2O$
	500	16.5	6CO
	560	2.8	CO
	950	21.7	$5CO_2$
11	145	11.0	$H_2O + 2CO_2$
	192	3.0	CO
	355	15.0	$9H_2O$
	482	16.0	6CO
	745	8.0	3CO
	935	13.5	5CO
16	167	4.0	$2H_2O$
	255	17.0	$4CO_2$
	350	13.0	$8H_2O$
	510	30.0	11CO
	870	4.0	CO_2

ligand, indirectly indicating the utilisation of the oxidised ligands in the formation of the final Cr^{III} products. Single crystal X-ray data obtained for crystals of the white solids obtained in the formation reactions of **2** and **3** were in agreement with previously reported data[25] for the corresponding ligands. Carbon-13 NMR spectra of complexes **1** and **3** showed evidence for the presence of carboxylate functions (δ 181 ± 1) as noted earlier.[20] The present study also suggests several common features among the structures of these complexes (**1**–**8**) and those obtained from the reaction of chromate with gluconic acid and galacturonic acid.

(*e*) *Thermogravimetric Analysis.*—Thermogravimetric analyses of compounds **1**, **4**, **5**, **10**, **11** and **16** were performed under an N_2 atmosphere and the results are shown in Table 3. The overall weight loss of these compounds is in the range 50–70% which corresponds to the loss of organic matter in the form of H_2O, CO or CO_2. The loss of CO_2 at relatively low temperatures lends further support to the complexes possessing carboxylate groups, though the number of these groups varies from compound to compound.

(*f*) *Magnetic Studies.*—Room-temperature magnetic susceptibility measurements on **1**–**8** gave μ_{eff} values (Table 2) comparable with those calculated for dinuclear Cr^{III} complexes. For **2**, **3**, **6** and **7**, measurements were performed as a function of

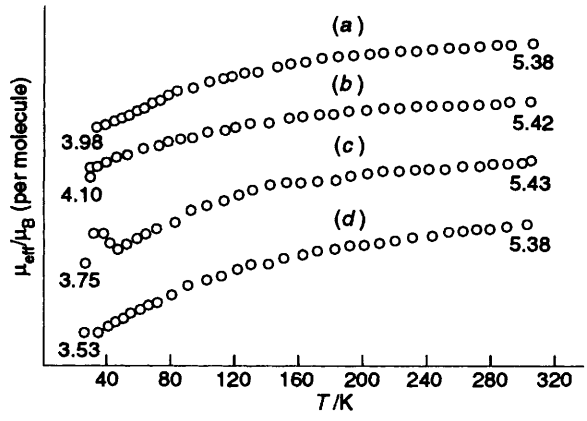

Fig. 2 Plot of μ_{eff} *vs.* *T* for **2** (*a*), **3** (*b*), **6** (*c*) and **7** (*d*)

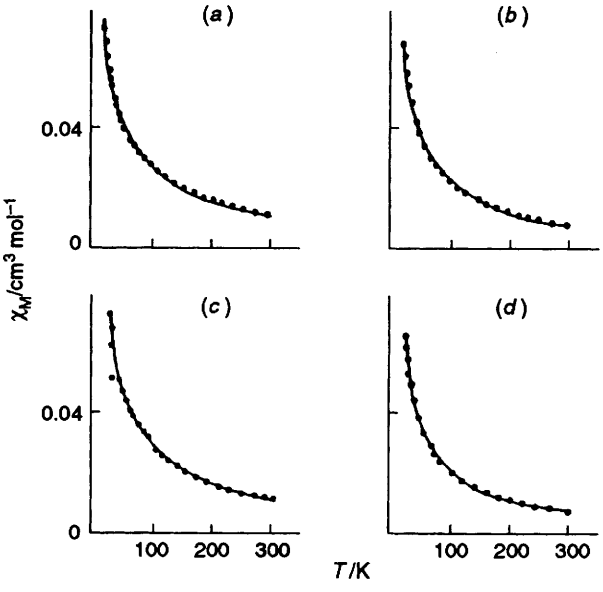

Fig. 3 Plot of χ_M *vs.* *T*, (●) experimental points, (—) theoretical fitting, for (*a*) **2** (p = 0.03), (*b*) **3** (p = 0.01), (*c*) **6** (p = 0.02) and (*d*) **7** (p = 0.12)

temperature, from room temperature down to 24 K using liquid helium. All the complexes exhibited non-linear behaviour for $1/\chi_g$ *vs.* *T* upon cooling with a substantial decrease in μ_{eff} (in the range 26–35%). This suggests an antiferromagnetic interaction between the two Cr^{III} centres (Fig. 2). The data for these four complexes have been analysed on the basis of the usual spin–spin interaction model with the exchange Hamiltonian, $\mathcal{H} = -2JS_1 \cdot S_2$, $S_1 = S_2 = \frac{3}{2}$, $g = 1.98$ and t.i.p. (temperature-independent paramagnetism) = 0. The magnetic susceptibility expressions are given in equations (1) and (2), where $x =$

$$\chi' = \frac{Ng^2\mu_B^2}{kT} \cdot \frac{[2e^x + 10e^{3x} + 28e^{6x}]}{[1 + 3e^x + 5e^{3x} + 7e^{6x}]} \quad (1)$$

$$\chi_m = \chi'(1 - p) + Ng^2\mu_B^2 S(S + 1)p/3kT + \text{t.i.p.} \quad (2)$$

$2J/kT$, p is the fraction of the magnetic impurity, and all other parameters have their usual meaning.

The magnetic data were fitted by a non-linear least-squares procedure to yield $-2J$ values of 13.6, 10.0, 15.0 and 20.0 cm^{-1}, respectively (Fig. 3). The dihydroxo-bridged complex[26] $[(tmpa)Cr(\mu\text{-}OH)_2Cr(tmpa)]^{4+}$ [where tmpa = tris(2-pyridylmethyl)amine] as well as the hydroxo- and carboxylato-bridged complex, $[LCr(OH)(MeCOO)_2CrL]^{3+}$ (where L = 1,4,7-trimethyl-1,4,7-triazacyclononane), showed $-2J$ values of about 31 cm^{-1}.[27] On the other hand, dinuclear Cr^{III} com-

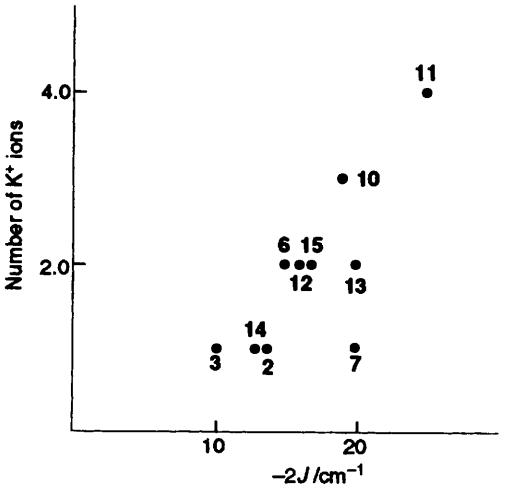

Fig. 4 Plot of $-2J$ *vs.* the number of K^+ ions

plexes with no bridging oxo or hydroxo groups, such as $Na_3[Cr_2(acac)_2\{(L\text{-tart})_2H\}]\cdot 7H_2O$, $H[Cr_2\{(L\text{-tart})_2H\}(bipy)_2]\cdot 3.5H_2O$ and $H[Cr_2\{(meso\text{-tart})_2H\}(bipy)_2]\cdot 6H_2O$ (tart = $C_4H_2O_6^{4-}$, acac = acetylacetonate and bipy = 2,2′-bipyridyl), exhibited weak ferromagnetic interactions between the Cr^{III} centres[28] which were bridged *via* the carboxylate group of the tartrate ligand. The plot of $-2J$ *vs.* the number of K^+ ions (see Table 5) showed a fairly linear trend (Fig. 4), with an increase in the number of K^+ ions being proportional to the increase in the antiferromagnetic coupling value. This clearly supports the presence of extensive intermolecular interactions as suggested by the EPR data and the solubility of the complexes.

(*g*) *Electrochemical Studies.—At a hanging-drop mercury electrode.* All complexes exhibited an irreversible cathodic peak assigned to Cr^{III}–Cr^{II} reduction (E_p^c) in cyclic voltammetric studies carried out in aqueous solution at HMDE. The E_p^c values were in the range -1.1 to -1.4 V depending upon the reductant (Table 4).

The E_p^c values were also found to be sensitive to pH. In the pH range 2–12 studied the complexes were hydrolytically stable, and the E_p^c values exhibited a fairly linear trend w.r.t. pH as shown in Fig. 5. The slopes of the lines (in mV per unit of pH) indicate the sensitivity of the overall structure of the complexes towards the pH of the environment, and decrease in the following order: complex **12** (55) > **10** (33) > **8** (32) > **16** (30) > **14** (26), **3** (26) ≥ **1** (25) ≥ **2** (24), **4** (24), **5** (24) ≥ **7** (23) > **11** (12) ≥ **13** (10), **6** (10) ≥ **15** (7). From these values the complexes can be divided into four categories: (*i*) complexes with a large slope of 55 mV per pH unit (complex **12**), (*ii*) those with values in the range 30–33 (av. 32 mV per pH unit) (**8**, **10** and **16**), (*iii*) those with slopes of 23–26 (av. 24 mV per pH unit) (**1**–**5**, **7** and **14**) and (*iv*) those with the lowest slopes in the range 7–12 (av. 10 mV per pH unit) (**6**, **11**, **13** and **15**). The differences in the slopes of categories (*ii*) and (*iii*) compared to (*iv*) are ascribed to the presence of monohydroxo bridges in the former two categories, and a dibridging hydroxo group in (*iv*). The rather small difference between the slopes of categories (*ii*) (three K^+) and (*iii*) (one K^+) is attributed to the number of counter cations present. The large perturbation observed for **12** may be explained in terms of the increased interaction of the carboxylate groups with increasing pH. Even in the case of the Cr^{III}–ATP complex **9** a single irreversible peak was observed at -1.342 V and the plot of E_p^c *vs.* pH gave a linear slope of 33 mV per pH unit. However, no formula was proposed for this complex owing to its hygroscopic nature.

All the complexes showed more negative potentials (E_p^c, Table 4) in non-aqueous solvents, with potentials becoming less

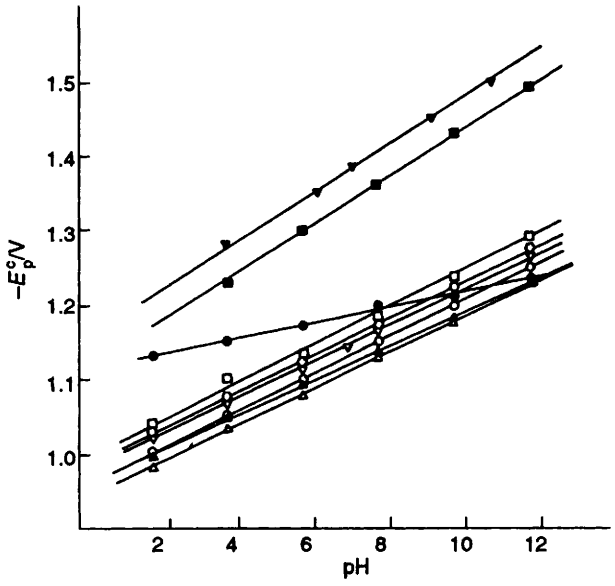

Fig. 5 Plot of the Cr^{III}–Cr^{II} reduction potential (E_p^c) as a function of pH for **1**–**9** at an HMDE working electrode, Ag–AgCl reference electrode, scan speed 0.1 V s^{-1}: complex **1** (○), **2** (△), **3** (□), **4** (▽), **5** (◯), **6** (●), **7** (▲), **8** (■) and **9** (▼)

Table 4 Chromium(III)–chromium(II) reduction potentials (E_p^c/V) for complexes **1**–**9** in different solvents at an HMDE

	Solvent			
Complex	H_2O	MeOH	MeCN	dmf
1	−1.150	−1.319	−1.456	−1.521
2	−1.144	−1.300	−1.395	−1.495
3	−1.156	−1.520	−1.564	−1.800
4	−1.141	−1.543	−1.640	−1.800
5	−1.170	−1.450	−1.665	−1.723
6	−1.190	−1.422	−1.690	−1.755
7	−1.123	−1.369	−1.400	−1.596
8	−1.360	−1.428	−1.451	−1.535
9	−1.342	—	—	—

negative in the order dmf > MeCN ≥ MeOH > H_2O. This suggests a direct involvement of the solvent in the co-ordination sphere of these complexes and not just a dielectric effect.

The Cr^{III}–Cr^{II} reduction potentials (at HMDE) are related to the overall negative charge of the complexes (Table 4). This is convincingly represented by a plot of the number of counter cations (K^+) *vs.* $-E_p^c$ for all the complexes **1**–**16** which gives a linear trend [Fig. 6(*a*)], with a shift of about 100 mV in E_p^c per increase of unit negative charge on the complex.

A plot of $-E_p^c$ *vs.* the reductive coefficient derived for a large number of reductants, details of which have been discussed previously[13] also showed a linear trend [Fig. 6(*b*)]. This suggests that the type of reductant used influences the nature of the final Cr^{III} complex formed, as expected.

At platinum in MeOH. The CV studies were also carried out using Pt as the working electrode in the range 1.0 to -1.5 V in MeOH. Typical voltammograms are shown in Fig. 7. In the range 0.0 to 1.0 V in most cases a single quasi-reversible and/or irreversible Cr^{III}–Cr^{IV} oxidation peak (E_p^a) was observed [Fig. 7(*e*)–(*h*)]. However, in other cases, namely for **3**, **4**, **8**, **12**, **14** and **15**, a second quasi-reversible oxidation couple was observed at more positive values. These observations indicate the formation of mixed valence (III, IV) and/or completely oxidised (IV, IV) species in solution under an argon atmosphere supporting the dinuclear nature of the complexes. Chromium(III) complexes are known to show quasi-reversible one-electron oxidation waves at Pt in the range 1.17–1.22 V (*vs.* the standard hydrogen

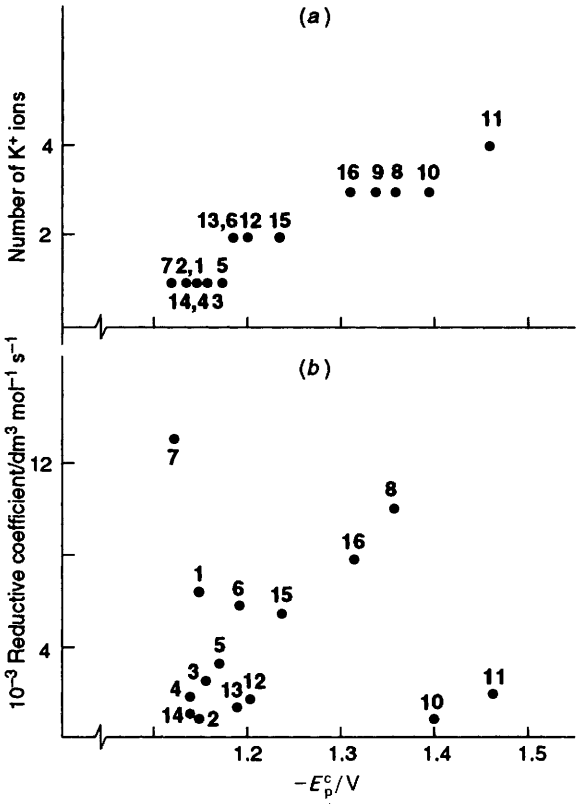

Fig. 6 Plots of (*a*) the number of K^+ counter ions and (*b*), the reductive coefficient ($dm^3\ mol^{-1}\ s^{-1}$) *vs.* $-E_p^c$ of complexes **1**–**16** at HMDE

electrode).[27] Even in the range 0.0 V to −1.4 V all the complexes showed two quasi-reversible and/or irreversible cathodic Cr^{III}–Cr^{II} reduction peaks (E_p^c) corresponding to the presence of two Cr^{III} centres [Fig. 7(*a*)–(*d*)].

The E_p^a values were found to decrease with increasing number of K^+ counter ions (overall negative charge on the complex) [Fig. 8(*a*)] indicating that the oxidation is easier for the complexes with higher negative charge. A linear slope was also observed for a plot of $-E_p^c$ *vs.* the number of K^+ ions [Fig. 8(*b*)], with an opposite sign to Fig. 8(*a*), as expected for the reduction process.

Plots of $-E_p^c$ [Fig. 9(*a*)] or E_p^a [Fig. 9(*b*)] *vs.* $-2J$ also showed linear trends with opposite slope signs as expected indicating that the Cr^{III} centres are indeed involved in influencing the magnetic interactions.

(*h*) *The Nature of the Products.*—The final Cr^{III} saccharide and related products are found to be anionic with Cr^{III} exhibiting pseudo-octahedral geometry as shown by various studies. The metal centre is bound to both the oxidised and unoxidised ligands. Evidence for the presence of bound oxidised moieties through carboxylate functions in the co-ordination sphere mainly lies in the ^{13}C NMR spectral data further supported by FTIR spectra. All the complexes showed weak antiferromagnetic interactions between the two Cr^{III} centres. The fact that, even at very low pH (0.5), the complexes do not show any indication of protonation of the species (based on the absorption measurements), suggests that they are hydrolytically stable and also supports the presence of hydroxo bridging in these complexes, as derived from magnetic studies. In the reduction of Cr^{VI} by saccharides and their derivatives to form Cr^{III} saccharide complexes, the presence of OH on C^2 of the saccharide chain was found to be important in supporting the involvement of C^2–O^- in co-ordination.[13] Furthermore, the EXAFS studies carried out on iron saccharide complexes suggested bidentate co-ordination of the saccharides.[29] From photochemical studies on saccharides in the presence of iron, it

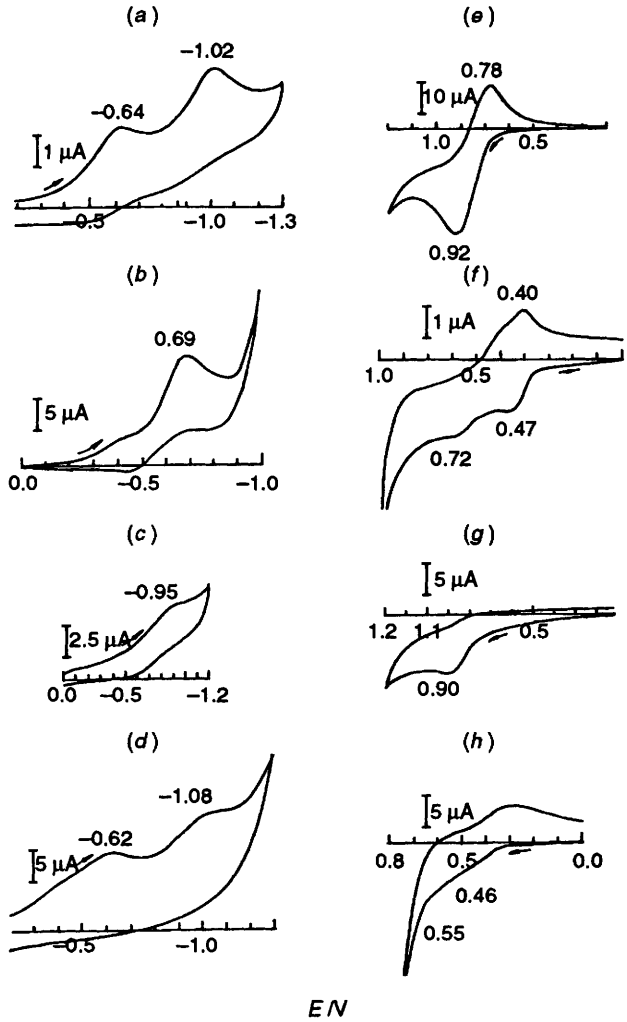

Fig. 7 Cyclic voltammograms of **2** (*a*) and (*e*), **4** (*b*) and (*f*), **6** (*c*) and (*g*) and **8** (*d*) and (*h*) in MeOH at Pt, in 0.1 mol dm^{-3} NMe_4Cl, Ag–AgCl reference electrode, scan speed 0.1 V s^{-1}

was reported that C^2 and C^3 hydroxyl groups of the saccharide bind to the iron.[30] Accordingly, the observed analytical results (see Experimental section) have been interpreted to provide proposed structures for the final Cr^{III} products of the chromate reduction process and are given in Table 5 with, schematic sketches of **1** and **3** shown in Fig. 10. Both the CV data for Cr^{III}–Cr^{II} reduction and the ionic conductivities are in accord with the total negative charge on the complexes, and their *m*:*n* electrolyte behaviour, respectively. Also, the mono- and di-hydroxo bridging nature of the complexes is supported by CV studies at varying pH values with several correlations shown in Figs. 1, 6, 8 and 9 further supporting the proposed formulae. However, the present data cannot unambiguously delineate the bridging role of the OH and carboxylate functions in these complexes in the absence of crystal structure determinations and/or labelling studies. Various attempts to crystallise the complexes have so far been unsuccessful.

(*i*) *Interaction of Complexes* **1** *and* **3** *with DNA.*—The reactivity of complexes **1** and **3** with pSV_2neo plasmid DNA was studied by agarose-gel electrophoresis. The DNA sample is predominantly in the nicked form (form II) with only a small proportion of super-coiled form (form I) and was incubated with different concentrations of **1**. As the concentration of the complex was increased there was an increase in the amount of the linear form, a decrease in the nicked form and disappearance of the super-coiled form. This suggests that upon

the interaction of **1** with DNA the nicked form is converted to the linear form and the super-coiled form to the nicked form. Qualitatively similar trends were noted for **3**. Similar studies were also carried out on the Cr^{III} complexes of D-galacturonic and D-gluconic acids (**15** and **16**).[20] While at low Cr^{III} concentration these complexes showed similar characteristics to **1** and **3**, at higher concentration only a smear of the DNA band was observed indicating further fragmentation of the DNA.

In vitro studies between a Cr^{V} complex and a covalently closed circular plasmid DNA revealed that Cr^{V} cleaves DNA through a ligand-exchange reaction.[3] Ligand exchange has also been noted in solution from the incipiently formed Cr^{III} complex in the *in vitro* reduction of chromate by L-cysteine

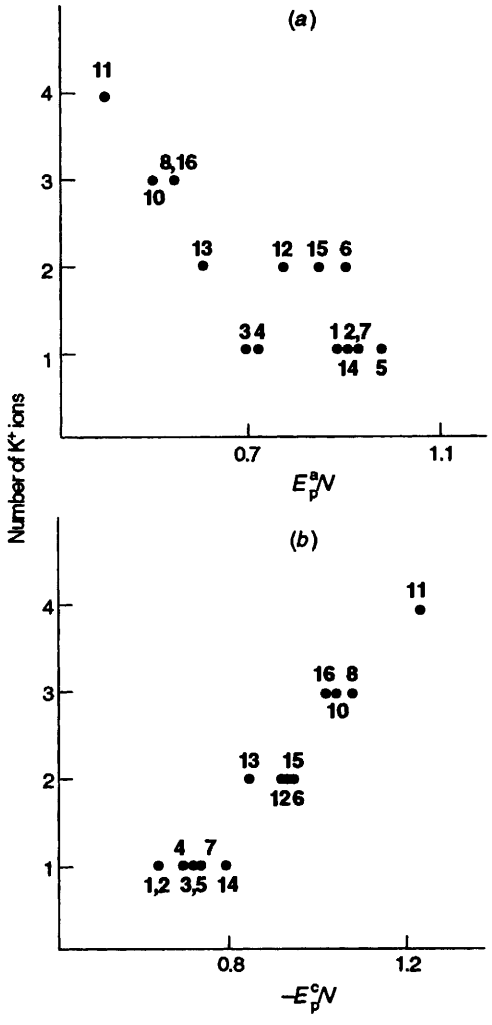

Fig. 8 Plots of the number of K^+ counter ions *vs.* E_p^a (*a*) and $-E_p^c$ (*b*) in MeOH at Pt working electrode

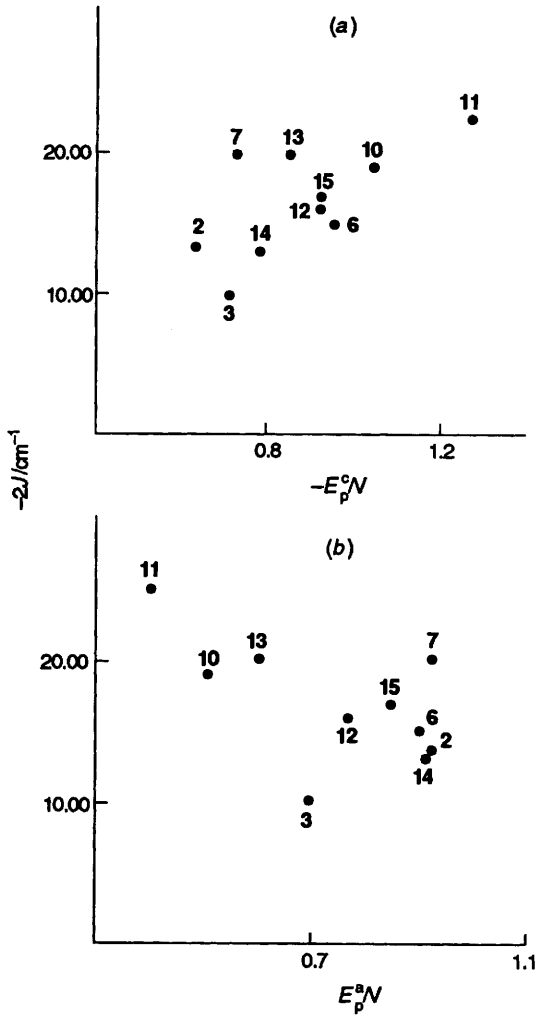

Fig. 9 Plots of $-2J$ *vs.* $-E_p^c$ (*a*) and E_p^a (*b*)

Table 5 Proposed structural formulae, conductivity data and antiferromagnetic coupling constants for the Cr^{III} complexes*

Complex	Structural formula	Molecular conductivity/ $ohm^{-1}\ cm^2\ mol^{-1}$	$-2J/cm^{-1}$
1	$K[Cr_2(\mu\text{-}OH)(D\text{-}Rib)_2(D\text{-}Rib')_2]\cdot 2H_2O$	62	—
2	$K[Cr_2(\mu\text{-}OH)(D\text{-}Xyl)_2(D\text{-}Xyl')_2]\cdot H_2O$	72	13.6
3	$K[Cr_2(\mu\text{-}OH)(D\text{-}Lac')_2]\cdot 2H_2O$	56	10.0
4	$K[Cr_2(\mu\text{-}OH)(D\text{-}Mal')_2]\cdot H_2O$	53	—
5	$K[Cr_2(\mu\text{-}OH)(edo')_4]\cdot 3H_2O$	52	—
6	$K_2[Cr_2(pto)_2(pto')_4]\cdot H_2O$	105	15.0
7	$K[Cr_2(\mu\text{-}OH)(Man\text{-}ol)_2(Man\text{-}ol')_2]\cdot 3H_2O$	64	20.0
8	$K_3[Cr_3(\mu\text{-}OH)(dha)_3(dha')_3]\cdot 4H_2O$	165	—
10	$K_3[Cr_2(\mu\text{-}OH)(D\text{-}Glc)_2(D\text{-}Glc')_2]\cdot 2H_2O$	158	19.0
11	$K_4[Cr_2(\mu\text{-}OH)_2(D\text{-}Fru)_2(D\text{-}Fru')_2]\cdot H_2O$	240	25.0
12	$K_2[Cr_2(\mu\text{-}OH)_2(D\text{-}Gal')_4]\cdot 2H_2O$	126	16.0
13	$K_2[Cr_2(\mu\text{-}OH)_2(D\text{-}Man)_2(D\text{-}Man')_2]\cdot 4H_2O$	123	20.0
14	$K[Cr_2(\mu\text{-}OH)(L\text{-}Sor')_2]\cdot 2H_2O$	68	13.0
15	$K_2[Cr_2(\mu\text{-}OH)_2(D\text{-}GalA)_4]\cdot 1.5H_2O$	115	16.8
16	$KNa_2[Cr_2(\mu\text{-}OH)(D\text{-}Glc\text{-}onic)_4]\cdot 2H_2O$	174	—

* Primes indicate oxidised forms of the ligands. The abbreviations employed for the saccharides represent anionic forms.

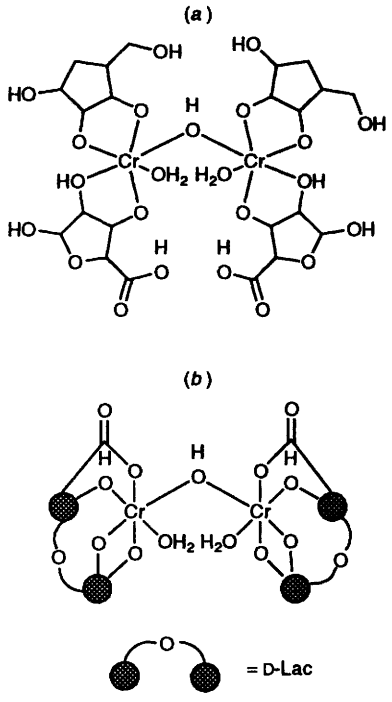

Fig. 10 Proposed structures for the Cr^{III}–D-Rib complex **1** (*a*) and the Cr^{III}–D-lactose complex **3** (*b*)

and some SH-containing molecules.[31] Wetterhahn and co-workers[32] have also shown that the activation of Cr^{VI} by thiols results in the formation of Cr^{V} which in turn interacts with the plasmid pBR322 and alters the conformation of DNA. Although most previously reported studies implicate Cr^{V} as a likely cause of DNA damage, our studies on the Cr^{III} complexes, **1**, **3**, **10**, **11** and **13**–**16**, have shown changes in the DNA structure. Therefore, extending these results to a cellular context, it is tempting to suggest that the Cr^{III} products generated by chromate reduction inside the cell may further interact with DNA. In fact, Costa and co-workers[33] have shown that Cr^{III} may participate in the formation of DNA–protein complexes isolated from cultured Chinese hamster ovary cells treated with Cr^{VI}. This gives a real impetus to carry out more detailed studies to understand the mechanism of the interaction of these complexes with DNA.

(*j*) *Implications.*—All the Cr^{III} complexes that have been isolated so far from the reaction of chromate with saccharides and their derivatives have been dinuclear. As both Cr^{III} and the intermediate Cr^{V} are capable of exchanging and expanding their co-ordination sphere, it may be implied that the polygalacturonic acids present in the plant roots can absorb chromium from such complexes. The hydrolytically stable nature of these complexes over a wide pH range suggests that the facile transport of such complexes through soil should be possible, before the chromium ions are absorbed or hydrolysed to form insoluble hydroxides. As the Cr^{III} complexes generated by chromate reduction have bound hydroxyl and carboxylate groups, it may be that the humic and fulvic components of soil operate in the same manner, resulting in the solubilisation, transport and absorption of chromium in the environment.

Acknowledgements

We thank the Department of Science and Technology (DST) and Council for Scientific and Industrial Research (CSIR), New Delhi, for financial support. The BAS100B electrochemical analyser was purchased from DST funds. S. P. K. is grateful to CSIR for the award of senior research fellow. We thank Professor S. Mitra, Tata Institute of Fundamental Research, Bombay, Dr. P. Chaudhari, Ruhr University and Dr. N. Y. Vasanthacharya, Indian Institute of Science Bangalore for the variable-temperature magnetic susceptibility data. We also thank the Regional Sophisticated Instrumentation Centre, Indian Institute of Technology, Bombay for NMR, FTIR, EPR and ICP-AES data. We thank Dr. K. K. Rao of our Institute for the sample of pSV2neo plasmid.

References

1 J. D. Nriagu and E. Nieboer, *Adv. Environ. Sci. Technol.*, 1988, **1**, 1.
2 P. H. Connett and K. E. Wetterhahn, *Struct. Bonding (Berlin)*, 1983, **54**, 93.
3 R. P. Farrell and P. A. Lay, *Comments Inorg. Chem.*, 1992, **13**, 133.
4 C. F. G. C. Geraldes and M. M. C. A. Castro, NATO ASI Series G, 1990, vol. 23, p. 105 and refs. therein.
5 H. A. T. Riahi, *J. Inorg. Biochem.*, 1990, **39**, 33.
6 D. M. Whitfield, S. Stojkovski and B. Sarkar, *Coord. Chem. Rev.*, 1993, **122**, 171 and refs. therein.
7 S. Yano, *Coord. Chem. Rev.*, 1988, **92**, 113.
8 S. J. Angyal and D. C. Graig, *Carbohydr. Res.*, 1993, **241**, 1.
9 K. Burger and L. Nagy, *Biocoordination Chemistry*, ed. K. Burger, Ellis Horwood, New York, 1990, p. 236.
10 S. Agarwal, H. P. Tiwari and J. P. Sharma, *Tetrahedron*, 1990, **46**, 1963.
11 C. P. Rao, P. S. Sarkar, S. P. Kaiwar and S. Vasudevan, *Proc. Ind. Acad. Sci. (Chem. Sci.)*, 1990, **102**, 219.
12 C. P. Rao and S. P. Kaiwar, *Carbohydr. Res.*, 1992, **237**, 195.
13 C. P. Rao and S. P. Kaiwar, *Carbohydr. Res.*, 1993, **244**, 15.
14 C. P. Rao and S. P. Kaiwar, *Inorg. Chim. Acta*, 1991, **186**, 11.
15 C. P. Rao, K. Geetha and R. P. Bandwar, *Bioorg. Med. Chem. Lett.*, 1992, **2**, 997.
16 S. P. Kaiwar and C. P. Rao, *Carbohydr. Res.*, 1992, **237**, 203.
17 C. P. Rao, K. Geetha and M. S. S. Raghavan, *BioMetals*, 1994, **7**, 25.
18 S. P. Kaiwar, M. S. S. Raghavan and C. P. Rao, *Carbohydr. Res.*, 1994, **256**, 29.
19 S. P. Kaiwar and C. P. Rao, *Chem.-Biol. Interact.*, 1995, in the press.
20 C. P. Rao, S. P. Kaiwar and M. S. S. Raghavan, *Polyhedron*, 1994, **13**, 1895.
21 L. G. Marzilli, *Adv. Inorg. Biochem.*, 1981, **3**, 47.
22 H. A. T. Riahi, *Carbohydr. Res.*, 1988, **183**, 35.
23 A. M. Calafat, J. J. Fiol, A. Terron, V. Moreno, D. M. L. Goodgame and I. Hussain, *Inorg. Chim. Acta*, 1990, **169**, 133 and refs. therein.
24 L. Nagy, K. Burger, J. Kurti, M. A. Mostafa, L. Koresz and I. Kiricsi, *Inorg. Chim. Acta*, 1986, **124**, 55.
25 S. Takagi and G. A. Jeffrey, *Acta Crystallogr., Sect. B*, 1979, **35**, 1482; D. C. Fries, S. T. Rao and M. Sundaralingam, *Acta Crystallogr., Sect. B*, 1971, **27**, 994; C. A. Beevers and H. N. Hansen, *Acta Crystallogr., Sect. B*, 1971, **27**, 1323.
26 P. Chaudhuri, M. Winter, H. -J. Kuppers, K. Wieghardt, B. Nuber and J. Weiss, *Inorg. Chem.*, 1987, **26**, 3302.
27 B. G. Gafford, R. E. Marsh, W. P. Schaefer, J. H. Zhang, C. J. O'Connor and R. A. Holwerda, *Inorg. Chem.*, 1990, **29**, 4652.
28 M. Nakahanda, T. Fujihara, N. Koine and S. Kaizeaki, *J. Chem. Soc., Dalton Trans.*, 1992, 3423.
29 L. Nagy, H. Ohtaki, H. Yamaguchi and M. Nomura, *Inorg. Chim. Acta*, 1989, **159**, 201.
30 K. Araki and S. Shiraishi, *Bull. Chem. Soc. Jpn.*, 1986, **59**, 229.
31 S. P. Kaiwar, Ph. D. Thesis, Indian Institute of Technology, Bombay, 1994.
32 K. M. Borges, J. S. Boswell, R. H. Liebross and K. E. Wetterhahn, *Carcinogenesis (London)*, 1991, **12**, 551.
33 X. Lin, Z. Zhuang and M. Costa, *Carcinogenesis (London)*, 1992, **13**, 1763.

Received 29*th June* 1994; *Paper* 4/03955I